REPORT DOCUMENTATION PAGE

Form Approved
OMB No. 0704-0188

1. REPORT DATE *(DD-MM-YYYY)*	2. REPORT TYPE	3. DATES COVERED *(From - To)*
30-April-2015	Final Technical Report	1-Nov-2013 - 31-Jan-2015

4. TITLE AND SUBTITLE

Hydrodynamic Drag Reduction

5a. CONTRACT NUMBER

5b. GRANT NUMBER
N00014-14-1-0103

5c. PROGRAM ELEMENT NUMBER

6. AUTHOR(S)

Dr. Lafe Taylor, Dr. Robert Wilson, Mr. Bruce Hilbert

5d. PROJECT NUMBER
14PR05745-01

5e. TASK NUMBER

5f. WORK UNIT NUMBER

7. PERFORMING ORGANIZATION NAME(S) AND ADDRESS(ES)

The University of Tennessee
at Chattanooga
615 McCallie Avenue
Chattanooga, TN 37403-2504

8. PERFORMING ORGANIZATION REPORT NUMBER

9. SPONSORING / MONITORING AGENCY NAME(S) AND ADDRESS(ES)

10. SPONSOR/MONITOR'S ACRONYM(S)

11. SPONSOR/MONITOR'S REPORT NUMBER(S)

12. DISTRIBUTION / AVAILABILITY STATEMENT

Distribution Statement A: Approved for Public Release; distribution is unlimited

13. SUPPLEMENTARY NOTES

14. ABSTRACT

National Center for Computational Engineering (SimCenter), University of Tennessee at Chattanooga, focused on the development of a computational procedure to evaluate various drag reduction strategies for hydrodynamically bluff-body vehicles. In particular, towards hydrodynamic drag reduction, different bow designs were investigated to replace the existing extendable bow vane of the current EFV configuration (designated as the Baseline ACV configuration in this report).

The *challenges* in this study and the *imposed constraints* to it were of particular note, as follows:

(1) As determined in a previous physical model-based assessment by the Naval Surface Warfare Center (NSWC), Carderock, in the "hump" region of total drag, generally, *only* about 6% of the total hydrodynamic drag of the Baseline ACV (*i.e.*, the current EFV) is due to friction; and the remaining 94% is largely *form drag*, together with wave drag. This is a very large departure from a ship hull designed from hydrodynamic drag considerations – for which, roughly 70% of the total drag would be due to friction, and the remainder would be the aggregate of form drag and wave drag. For the Baseline ACV, therefore, a measurable reduction of form drag was needed towards a reduction of total drag.

(2) The principal constraint imposed by the research sponsor was that *no* modifications to the hull shape could be made aft of the bow shoulders, *i.e.*, aft of the leading edge of the track channel. (This constraint was imposed so that different bow shapes could be "bolted on" at the shoulders of a physical model for towing-tank tests.) This implied that the box-like shape of nearly the entire hull (responsible for the extreme level of form drag) could *not* be altered. Without this constraint, a large improvement in total resistance could have been realized.

Subject to the above constraint, SimCenter's approach to the hull geometry modification can be summarized as below:

(a) Initially, various bow concepts were examined, while maintaining the original length of Baseline ACV with bow vane retracted. None of these concepts resulted in a measurable reduction in total resistance as compared to the baseline configuration. This was due to the imposed constraint described in (2) above. (Towing-tank test data for Baseline ACV model were used to validate the computational procedure.)

(b) The next step was to determine the minimum bow length necessary for a measurable reduction of the hull total resistance. Free surface viscous computations were performed for a number of candidate bow designs to determine their effectiveness in drag reduction. It was determined that, under the constraint described in (2) above, the minimum bow length required for an appreciable decrease in resistance was two feet (model scale), *as measured from the fore end of the track channel*. This actually translates to an approximate length *decrease* of one foot as compared to Baseline ACV with its bow vane deployed.

(c) This approach resulted in two promising designs, referred to as UTC 1 and UTC 2 in this report. These designs resulted in an average drag reduction of 9.2% and 8.1%, respectively, over the "hump" region.

(d) It should be noted that, although the overall length of UTC 1 and UTC 2 is greater than that of Baseline ACV, the static waterline lengths of UTC 1 and UTC 2 are actually *less than that of Baseline ACV with bow vane deployed*, by 11% and 14% respectively. This is due to the shaping of the bow, together with the fact that, for the same estimated payload, the drafts of UTC 1 and UTC 2 are less than that of Baseline ACV.

(e) Calculations of the lift force and trim moment imbalances for UTC 1 and UTC 2 show that the computational models will tend to sink slightly and rotate bow down to achieve dynamic equilibrium, relative to the baseline orientation. This could further reduce drag in the "hump" region.

It is recommended that a more comprehensive study of modifying the current vehicle be undertaken *removing* the restriction of no geometric modifications aft of the bow shoulders to determine to what extent the overall drag could be reduced using traditional naval architecture principles. *As stated previously, without this imposed restriction, a large improvement in total resistance could have been realized.*

15. SUBJECT TERMS

Physics-based simulation, viscous free surface, hybrid RANS/LES, bluff-body flow, drag reduction

16. SECURITY CLASSIFICATION OF:			17. LIMITATION OF ABSTRACT	18. NUMBER OF PAGES	19a. NAME OF RESPONSIBLE PERSON
a. REPORT	b. ABSTRACT	c. THIS PAGE			Dr. Lafe Taylor
U	U	U	SAR	21	19b. TELEPHONE NUMBER *(include area code)* (423) 425-5508

Final Technical Report

ONR Award No.: N00014-14-1-0103
Period of Performance: 01 Nov. 2013 – 31 Jan. 2015

Hydrodynamic Drag Reduction

Submitted by

Dr. Lafe Taylor
Email: Lafe-Taylor@utc.edu
Tel: (423) 425-5508

Dr. Robert Wilson
Email: Robert-Wilson@utc.edu
Tel: (423) 425-5433

Bruce Hilbert
Email: Bruce-Hilbert@utc.edu
Tel: (423) 425-5495

SimCenter: National Center for Computational Engineering
University of Tennessee at Chattanooga
701 East M.L. King Boulevard
Chattanooga, TN 37403

to

Jeffrey A. Bradel

Office of Naval Research
875 North Randolph Street
Arlington, VA 22203-1995
Email: JEFF.BRADEL@NAVY.MIL
Tel: (703) 588-2552

April 2015

TABLE OF CONTENTS

ABSTRACT

National Center for Computational Engineering (SimCenter), University of Tennessee at Chattanooga, focused on the development of a computational procedure to evaluate various drag reduction strategies for hydrodynamically bluff-body vehicles. In particular, towards hydrodynamic drag reduction, different bow designs were investigated to replace the existing extendable bow vane of the current EFV configuration (designated as the Baseline ACV configuration in this report).

The *challenges* in this study and the *imposed constraints* to it were of particular note, as follows:

(1) As determined in a previous physical model-based assessment by the Naval Surface Warfare Center (NSWC), Carderock, in the "hump" region of total drag, generally, *only* about 6% of the total hydrodynamic drag of the Baseline ACV (*i.e.*, the current EFV) is due to friction; and the remaining 94% is largely *form drag*, together with wave drag. This is a very large departure from a ship hull designed from hydrodynamic drag considerations – for which, roughly 70% of the total drag would be due to friction, and the remainder would be the aggregate of form drag and wave drag. For the Baseline ACV, therefore, a measurable reduction of form drag was needed towards a reduction of total drag.

(2) The principal constraint imposed by the research sponsor was that *no* modifications to the hull shape could be made aft of the bow shoulders, *i.e.*, aft of the leading edge of the track channel. (This constraint was imposed so that different bow shapes could be "bolted on" at the shoulders of a physical model for towing-tank tests.) This implied that the box-like shape of nearly the entire hull (responsible for the extreme level of form drag) could *not* be altered. Without this constraint, a large improvement in total resistance could have been realized.

Subject to the above constraint, SimCenter's approach to the hull geometry modification can be summarized as below:

(a) Initially, various bow concepts were examined, while maintaining the original length of Baseline ACV with bow vane retracted. None of these concepts resulted in a measurable reduction in total resistance as compared to the baseline configuration. This was due to the imposed constraint described in (2) above. (Towing-tank test data for Baseline ACV model were used to validate the computational procedure.)

(b) The next step was to determine the minimum bow length necessary for a measurable reduction of the hull total resistance. Free surface viscous computations were performed for a number of candidate bow designs to determine their effectiveness in drag reduction. It was determined that, under the constraint described in (2) above, the minimum bow length required for an appreciable decrease in resistance was two feet (model scale), *as measured from the fore end of the track channel*. This actually translates to an approximate length *decrease* of one foot as compared to Baseline ACV with its bow vane deployed.

(c) This approach resulted in two promising designs, referred to as UTC 1 and UTC 2 in this report. These designs resulted in an average drag reduction of 9.2% and 8.1%, respectively, over the "hump" region.

(d) It should be noted that, although the overall length of UTC 1 and UTC 2 is greater than that of Baseline ACV, the static waterline lengths of UTC 1 and UTC 2 are actually *less than that of Baseline ACV with bow vane deployed*, by 11% and 14% respectively. This is due to the shaping of the bow, together with the fact that, for the same estimated payload, the drafts of UTC 1 and UTC 2 are less than that of Baseline ACV.

(e) Calculations of the lift force and trim moment imbalances for UTC 1 and UTC 2 show that the computational models will tend to sink slightly and rotate bow down to achieve dynamic equilibrium, relative to the baseline orientation. This could further reduce drag in the "hump" region.

It is recommended that a more comprehensive study of modifying the current vehicle be undertaken *removing* the restriction of no geometric modifications aft of the bow shoulders to determine to what extent the overall drag could be reduced using traditional naval architecture principles. *As stated previously, without this imposed restriction, a large improvement in total resistance could have been realized.*

ADMINISTRATIVE INFORMATION

This work was initiated by Dr. Peter Majumdar, Chief Scientist, Marine Corps Systems Command and sponsored by the Office of Naval Research as part of the Science and Technology Expeditionary Maneuver Warfare and Combating Terrorism Program, ONR Code 30, with Jeffrey Bradel serving as project monitor.

1. BACKGROUND

The Amphibious Combat Vehicle (ACV) is a program initiated by the Marine Corps System Command to replace the Assault Amphibious Vehicle. In addition to design requirements for land-based operations, the ACV needs to be relatively compact so that a fleet can be transported to near-shore insertion points by Navy amphibious assault ships and subsequently travel at high rates of speed to safely reach the shore. The requirements of compact size and high payload for troop and equipment transport, results in the vehicle being bluff-shaped. Maximum horsepower requirements and engine size are then determined by the hydrodynamic performance of the hull in the so-called "hump-shaped" region of the resistance versus speed curve, which occurs at sub-planing speeds.

In the field of aerodynamics, Class 8 or semi-trucks historically have employed very inefficient shapes that are essentially bluff bodies. However, these designs have undergone a transformation in the last few years resulting in many of the newer models being much more streamlined and aerodynamically contoured because of the need to reduce drag, thereby increasing fuel efficiency and reducing operating costs. Increased fuel efficiency and reduced operating cost are the drivers of the quest to reduce overall drag on these vehicles. Whereas design procedures for streamlined, low-drag body shapes have improved, there is still work to be done for bluff body shapes that produce large regions of separated flow, especially when design constraints on maximum length and minimum volume prevent the use of slender, streamlined forms. Much of the improved aerodynamics of trucks has come from physics-based computational simulation methods and a similar approach can be taken for hydrodynamic marine vehicles. However, separated flows have proved to be a challenge with regard to computational fluid dynamics (CFD) simulations because of the difficulties encountered with the modeling of turbulence. Fortunately, models that employ Large Eddy Simulations (LES) or Detached Eddy Simulations (DES) have resulted in more realistic simulations in these regimes and thus played a key role in the efforts undertaken herein.

Unsteady DES aerodynamic simulations were performed at the SimCenter with the *Tenasi* flow code for the Generic Conventional Model (GCM), a 1:8 scale tractor–trailer model that was tested in the NASA Ames wind tunnel (Hyams et al., 2011). Computed pressure coefficients and drag force were in good agreement with measurements for a zero-incidence and 10 degree yaw cases. Unsteady incompressible flow simulations were performed for a modified full scale version of the GCM geometry to evaluate drag reduction devices. A simulation with trailer base flaps was also compared with drag reduction data from wind tunnels and track and road tests. A front spoiler and three mud flap designs with modest drag reduction potential was also evaluated.

Additional complications arise for simulation and design of hydrodynamic surface ships due to the presence of unsteady breaking waves with complex topologies and dense grid requirements to resolve small scales and large fluid property gradients across the air-water interface. Since the density ratio of water to air is 1000 to 1, the drag is dominated by the wetted hull surface. Unlike aerodynamic or fully submerged hydrodynamic vehicles, drag of surface ships at medium to higher speeds can be dictated by the wave component. As such, considerable effort in the bow design of surface ships is focused on the prevention of free surface build up, green water on deck, and large scale breaking waves in the axial direction, which directly increases drag.

Traditionally, this has been accomplished with V-shaped stepped, near surface bulbous and rearward slanting "tumble home" bow configurations for streamlined designs. However, due to the maximum length and minimum volume design constraints of the ACV, traditional bow concepts cannot be easily used and alternative strategies need to be explored. The focus of the current research is on identifying alternative ACV bow designs to decrease the so-called hump region of the resistance versus speed curve, which will facilitate the use of smaller, lighter engines.

2. COMPUTATIONAL METHODOLOGY

The SimCenter: National Center for Computational Engineering unstructured RANS/LES/DES solver, *Tenasi*, was used to predict drag and simulate the free surface flow around the ACV over a range of speeds. The software utilizes coarse-grained domain decomposition for scalable high performance parallel computing, artificial compressibility to enforce the pressure-velocity coupling, and a multiphase free surface capturing model for complex free surface topologies associated with high Froude number. The one-equation Spalart-Allmaras model is used for turbulence closure. Spatial discretization is accomplished by integrating the governing equations over a control volume surrounding each vertex, where the control volume is defined by median duals. Inviscid fluxes are evaluated using a second-order accurate Roe approximate Riemann scheme, while viscous fluxes are evaluated using a second-order directional derivative approach. The implicit time evolution algorithm uses Newton iterations to remove time linearization errors, where the primitive variables (pressure, velocity, and volume fraction) are updated simultaneously through the solution of a system of linear equations. A symmetric Gauss Seidel algorithm is used to solve the resulting linear system. A general multi-element unstructured control volume discretization is utilized to achieve resolution requirements for the free surface interface, near-wall viscous spacing for high Reynolds number flows, and complex geometry.

The unstructured surface capturing approach has been extensively validated for steady free surface flows at medium Froude numbers for the submerged NACA 0012 foil, the Wigley hull, and the Series 60 cargo ship, and the DTMB 5415 surface combatant (Nichols et al., 2002). It was later applied to high speed flow for the RV Athena I patrol ship with breaking bow and transom waves (Wilson et al, 2006) and was extended for simulating unsteady ship maneuvers (Wilson et al., 2007). Predictions of rigid body ship motions for the S175 container ship in incident waves and methodology for a one-way coupling of the Tenasi flow solver and the finite element code ABAQUS were presented, as well as results for flexure modal shapes, natural frequencies, and hull deformations (Wilson et al, 2008, Lee et al., 2008).

3. SIMULATION GEOMETRY, CONDITIONS, AND GRIDS

3.1 Geometry

A physical model of the full scale ACV vehicle (scale factor $L_{FS} / L_{MS} = 4.403$) was built and tested at NSWC-Carderock Division (NSWCCD). A computer-aided design (CAD) file specifying the baseline ACV geometry was provided by personnel at NSWCCD. Major components include the main hull with open track channels, retractable bow plate system with diamond, tractor system, track channel ballast plates, and adjustable transom flap. In an effort to

match the experimental weight and static condition of the physical model, the tractor system and ballast plates were removed, leaving an open track channel from bow to stern as shown in Figure 1. The specifications of the ACV baseline at model scale are summarized in Table 1, along with two new candidate designs, UTC 1 and UTC 2. Geometries for the three vehicles are shown in Figure 1 - Figure 4. Design strategies and specific differences between the baseline and candidate geometries are provided in Section 4.

Table 1. ACV baseline, UTC 1, and UTC 2 hull form characteristics at model scale

	Baseline	UTC 1	UTC 2
Static Waterline Length, L_{MS}	2.382 m (7.815 ft)	2.120 m (6.955 ft)	2.058 m (6.752 ft)
Draft, *D*	0.3599 m (1.1808 ft)	0.3086 m (1.0125 ft)	0.3190 m (1.0466 ft)
Beam, *B*	0.7978 m (2.6175 ft)	0.7978 m (2.6175 ft)	0.7978 m (2.6175 ft)
Displacement	4162.02 N (935.66 lbs)	4408.19 N (990.66 lbs)	4406.67 N (990.66 lbs)
Longitudinal CG, L_{CG} (forward of transom base)	0.8306 m (2.7251 ft)	-	-
Vertical CG, V_{CG} (above keel)	0.1025 m (0.3363 ft)	-	-

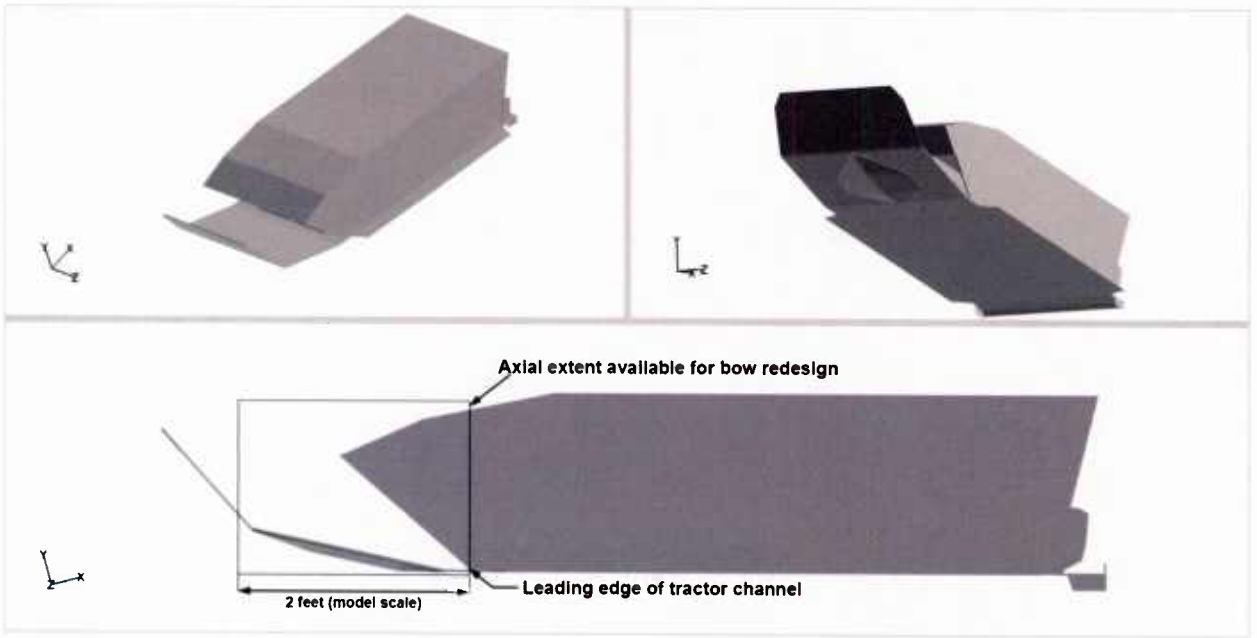

Figure 1. ACV baseline geometry

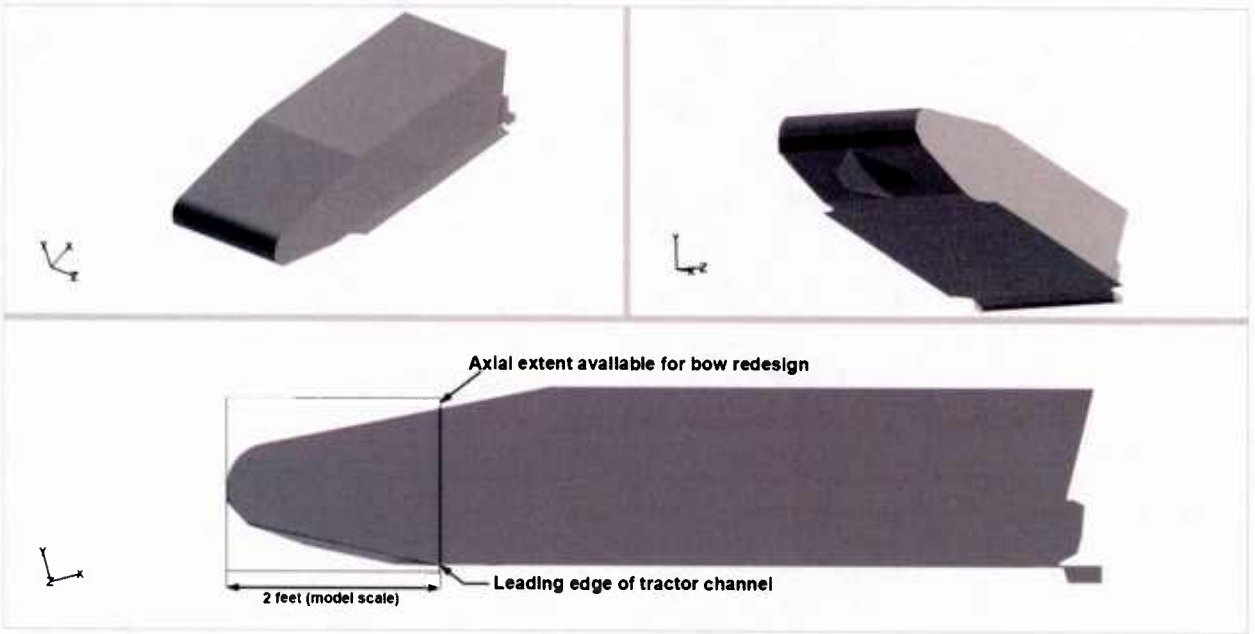

Figure 2. UTC 1 geometry

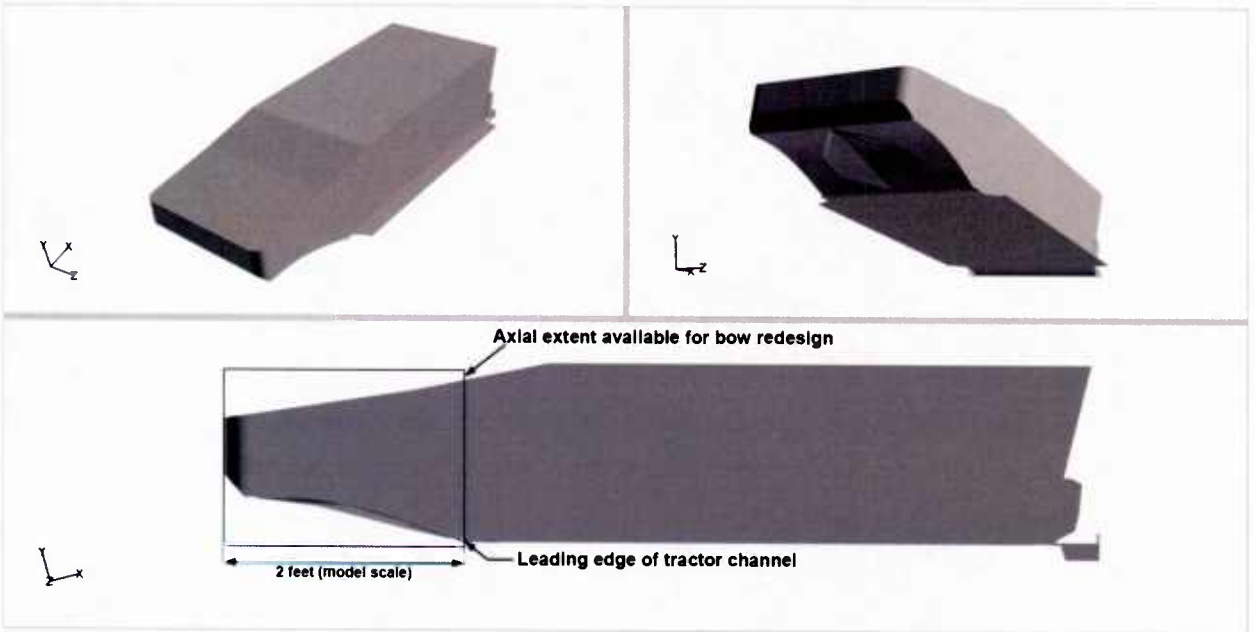

Figure 3. UTC 2 geometry

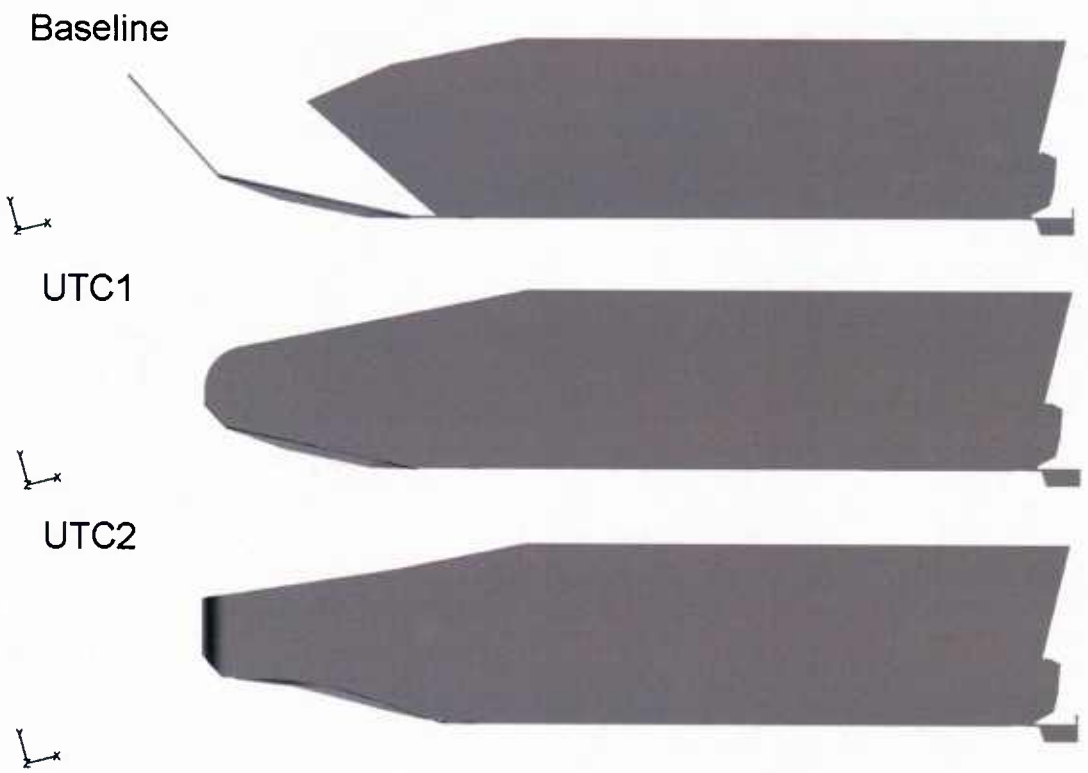

Figure 4. Profile comparisons for ACV geometries.

3.2 Conditions

The candidate designs UTC 1 and 2 feature closed bow sections, which effectively increase displacement for a given baseline, draft. It was estimated that the weight of closing the bow region would add approximately 55 lbs to the baseline model weight, resulting in the slightly heavier target displacement of 990.66 lbs for the new designs. In light of this, the draft for the new designs in static condition was then found by sinking the model until the target displacement was reached, resulting in a more shallow draft (88%D) compared to that of the baseline.

Free surface simulations for the baseline, UTC 1, and UTC 2 geometries were performed at model scale over a speed range from 6.08 to 25.73 full scale knots. For the baseline case, the hull orientation was fixed based on the measured equilibrium sinkage and trim over a range of speeds as provided by NSWCCD. For the redesigned bows, the trim was fixed at the measured baseline value, while the new sinkage $S_{UTC}(speed)$ was set by adding the difference in the static drafts of the UTC and baseline designs $(D_{UTC} - D_{BL})$ to the baseline sinkage $S_{BL}(speed)$ at the speed of interest

$$S_{UTC}(speed) = S_{BL}(speed) + [D_{UTC} - D_{BL}] \tag{1}$$

At the outer boundary, far-field characteristic-based boundary conditions are applied, while no-slip conditions are applied at the hull surface.

3.3 Grids

A composite overset grid approach was used in the simulation of ACV cases over a range of speeds and hull orientations. With this method, a body-fitted mesh was embedded in a fixed background mesh as shown in Figure 5. The body-fitted mesh was translated and rotated to match the target sinkage and trim for the speed of interest. The overset connectivity software Structured, Unstructured, Generalized Overset Assembler (SUGGAR) (Noack, 2005) was then used to compute donor and receptor information for intergrid transfers between the body-fitted and background grids in a preprocessing step. With this technique, the free surface interface is efficiently resolved and the body-fitted and background grids are generated once and used over a wide range of hull orientations. With a monolithic approach, the grid would need to be regenerated for each new speed.

All computational grids used in the project were created with the commercial meshing tool Pointwise (http://www.pointwise.com). The baseline, UTC 1, and UTC 2 geometries were imported and properly orientated as described above. A watertight surface grid consisting entirely of triangles was created for all three designs. The surface grid was constructed to respect the anisotropic spacing required by the air-water interface, as shown in Figure 6a for the baseline case and Figure 6b for UTC 1. This construction ensured that the mesh close to the surface met the same anisotropic requirement. The near surface viscous mesh was created using Pointwise's viscous layer prism/tetrahedral extrusion method, *T-Rex*. Near-wall spacing was specified to fully resolve the turbulent boundary layer to the wall and to satisfy turbulence modeling requirements ($y^+ = 1$). Finally, a structured background grid was constructed with a band of sufficiently dense spacing in the vertical direction to resolve the air-water interface. A summary of grid sizes is provided in Table 2.

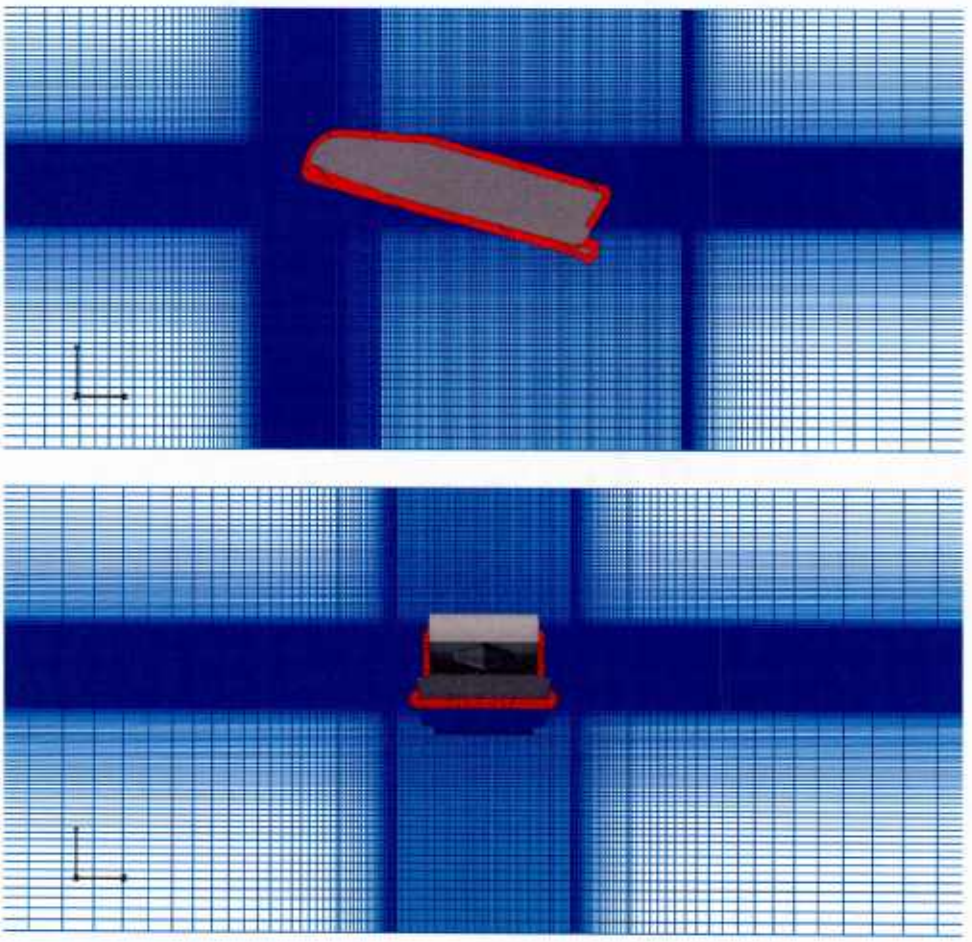

Figure 5. Overset grid system with center (top) and cross (bottom) plane details for body-fitted (red) and background (blue) meshes.

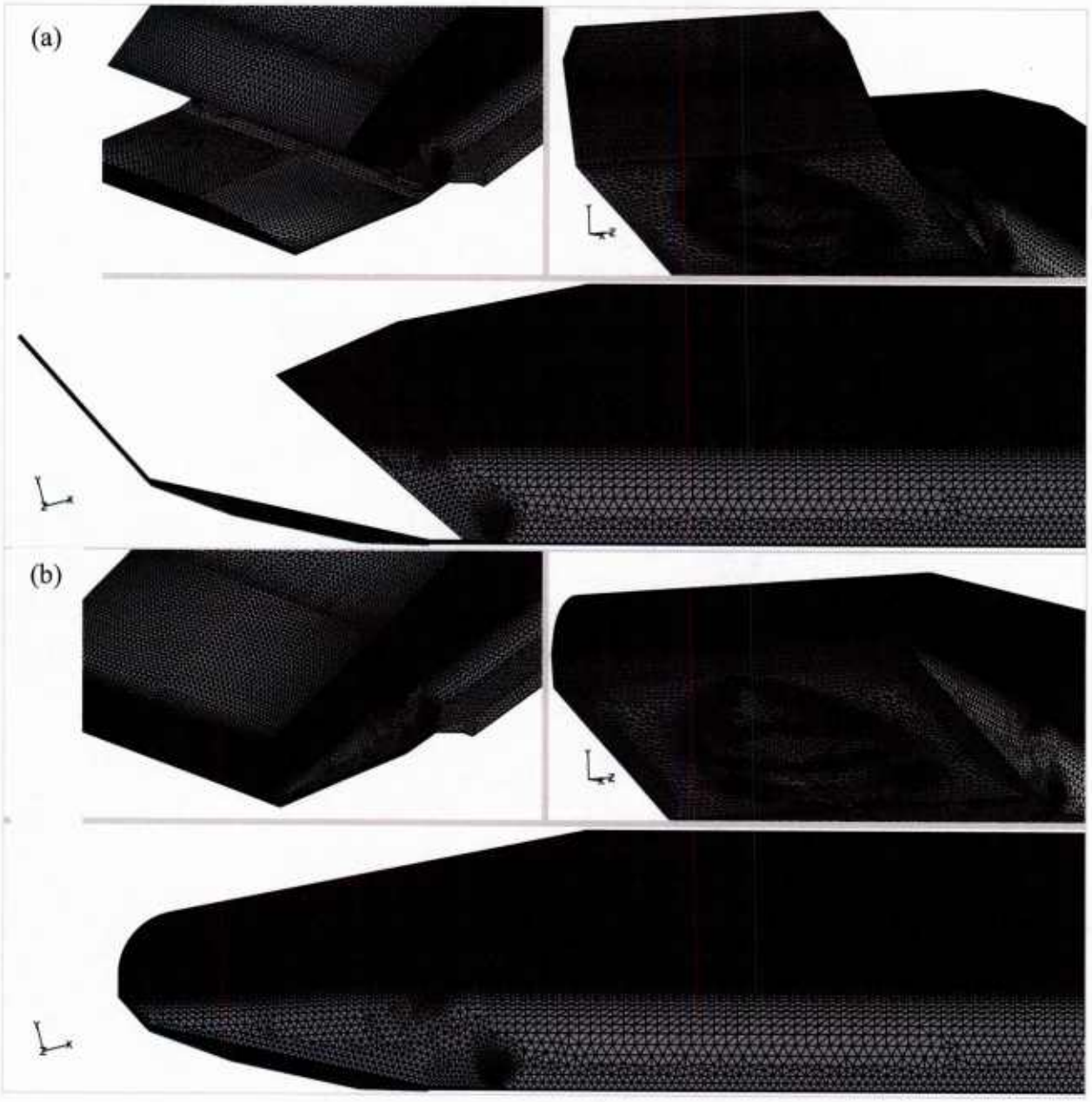

Figure 6. Surface mesh details for (a) ACV baseline and (b) UTC 1 cases.

Table 2. Grid dimensions for ACV simulations (all numbers in millions)

		Near-body	Background	Total
Baseline	nodes	4.98	24.7	29.7
	cells	10.7	24.5	35.2
UTC1	nodes	5.00	24.7	29.7
	cells	10.7	24.5	35.2
UTC2	nodes	5.19	24.7	29.9
	cells	11.2	24.5	35.7

4. DESIGN STRATEGY

The principal constraint imposed by the research sponsor was that *no* modifications to the hull shape could be made aft of the bow shoulders, *i.e.*, aft of the leading edge of the track channel. (This constraint was imposed so that different bow shapes could be "bolted on" at the shoulders of a physical model for towing-tank tests.) This implied that the box-like shape of nearly the entire hull (responsible for the extreme level of form drag) could *not* be altered. Without this constraint, a large improvement in total resistance could have been realized.

Subject to the above constraint, SimCenter's approach to the hull geometry modification can be summarized as below:

(a) Initially, various bow concepts were examined, while maintaining the original length of Baseline ACV with bow vane retracted. None of these concepts resulted in a measurable reduction in total resistance as compared to the baseline configuration. This was due to the imposed constraint described above. (Towing-tank test data for Baseline ACV model were used to validate the computational procedure.)

(b) The next step was to determine the minimum bow length necessary for a measurable reduction of the hull total resistance. Free surface viscous computations were performed for a number of candidate bow designs to determine their effectiveness in drag reduction. It was determined that, under the constraint described above, the minimum bow length required for an appreciable decrease in resistance was two feet (model scale), *as measured from the fore end of the track channel.* This actually translates to an approximate length *decrease* of one foot as compared to Baseline ACV with its bow vane deployed.

(c) This approach resulted in two promising designs, referred to as UTC 1 and UTC 2 and shown in Figure 2 and Figure 3, respectively. A comparison of profile shapes is provided in Figure 4.

With regard to UTC 1, the retracting bow plate system was replaced via a fixed section by closing the region between the main hull and the bow plates. The flat bottom section of UTC 1 is orientated at the same incident angle as the aft plate of the two-plate baseline bow system, while the portion of the forward plate that lies outside the design space is truncated. The static waterline length of the UTC 1 and 2 bow designs has actually decreased by 11% and 14%, respectively in comparison to the baseline value with bow plates deployed (i.e., operational mode) as shown in Table 1. With the baseline bow plates retracted (i.e., storage configuration), this modification effectively increases the baseline ship length from L_{MS}=1.96 m to 2.57 m. The modified designs move the longitudinal center of gravity forward and have the potential to favorably reduce the dynamic "squat", i.e., reduced sinkage and trim in the hump region so the ship will move to a planing condition sooner and with less horsepower.

With regard to UTC 2, the influence of the shape of the UTC 1 flat bottom plate on drag was first investigated by analyzing the surface force distribution in this region. Figure 8 shows a comparison of surface force distributions at $U_{FS}=14.90$ knots for baseline and UTC 1 simulations. Here, comparisons are made at equal sinkage and trim for the purpose of analysis, as

opposed to all other results, which were based on equal displacement in the static condition. It can be seen that the high force footprint for the baseline and UTC 1 cases are quite similar and limited to the forward section of the bottom bow plate. Since the drag force results from the axial component of the surface force vector, the flat bottom plate was redesigned with variable curvature to yield the UTC 2 concept. With this design, the incident angle is maximum at the aft end where the plate joins the main hull (Figure 4). Moving forward, the slope of the plate decreases and becomes horizontal at the forward end near the high force region. In other words, the axial component of the surface normal vector goes to zero and effectively reduces the drag on the bottom plate, as shown in Figure 8.

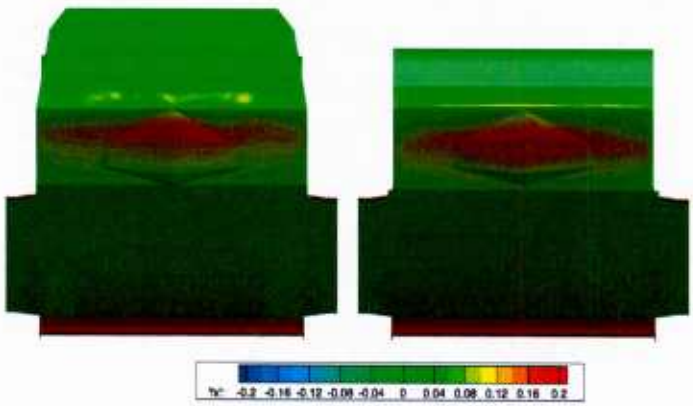

Figure 7. Surface distribution of drag force for baseline (left) and UTC 1 (right), $U_{FS} = 14.90$.

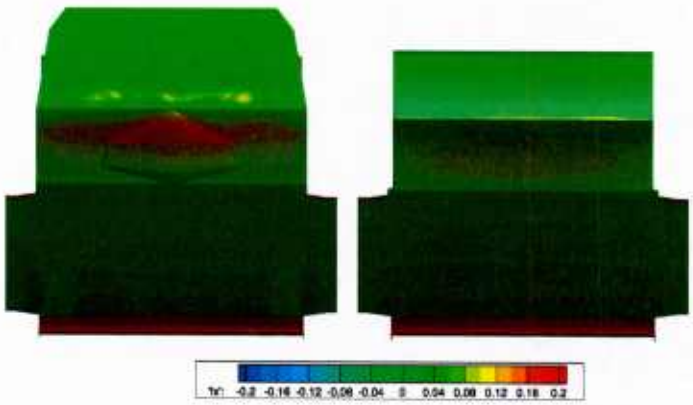

Figure 8. Surface distribution of drag for baseline (left) and UTC 2 (right), $U_{FS} = 14.90$.

5. RESULTS

5.1 Resistance

Predicted resistance values for the ACV simulations are compared to measurements of the baseline case over a range of speeds in Figure 9 and Table 3. Comparing the predicted and

measured values, it can be seen that the CFD results over predict the experimental values in the hump region from U_{FS}= 14.90 to 16.55 knots, with the largest difference (7%) at U_{FS} = 12.88. Differences at higher and lower speeds are much smaller (<1%).

Predictions for the UTC 1 design show drag reduction relative to the baseline CFD prediction of at least 7.5% over the entire hump region, with the maximum reduction of 11.2% at U_{FS} = 13.88. Drag reduction also occurs for the UTC 2 design over the entire hump region, with a maximum reduction of 12.8% at U_{FS} = 16.63. The maximum drag value has been shifted to a lower speed from U_{FS}= 13.88 to 12.88 knots.

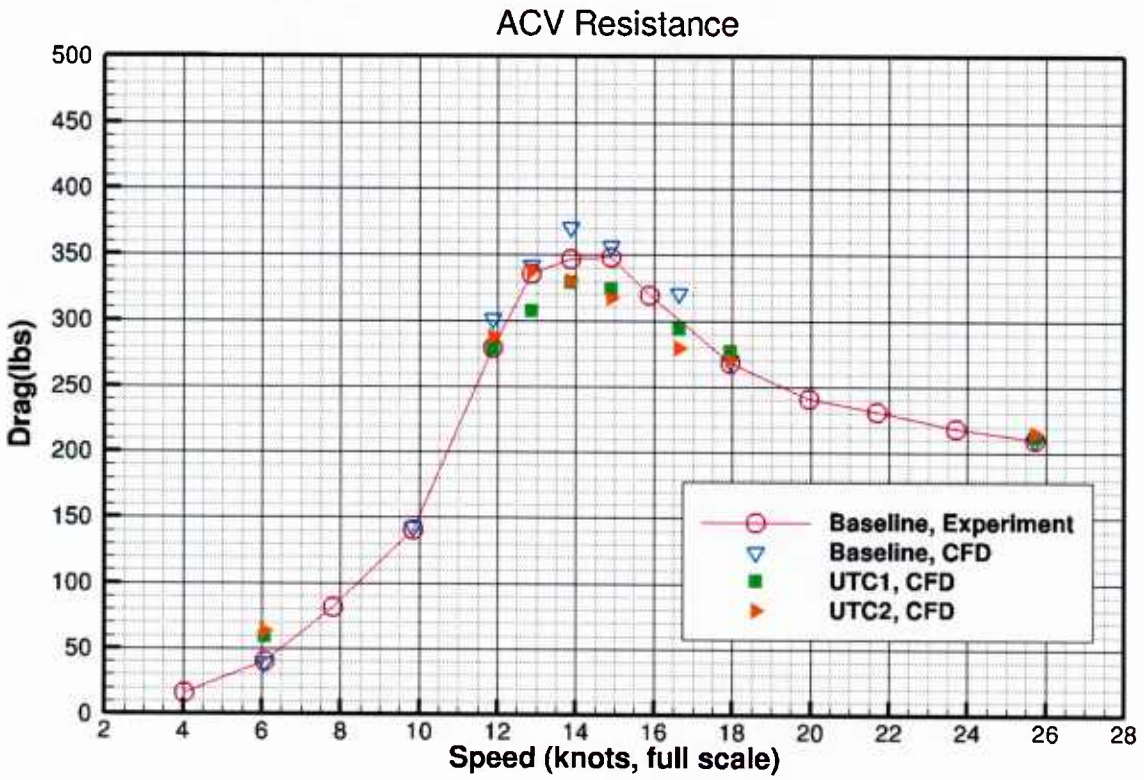

Figure 9. ACV resistance versus speed.

Note: Had it not been for the imposed design constraint (see paragraph labeled (2) on page 2), a large improvement in total resistance could have been realized.

Table 3. ACV resistance values in the hump region

U_{FS}	Baseline, Experiment	Baseline, CFD (difference)[1]	UTC 1, CFD (difference)[2]	UTC 2, CFD (difference)[2]
11.89	279.21	301.33 (+6.9%)	278.59 (-7.5%)	287.70 (-4.5%)
12.88	335.23	341.88 (+2.0%)	307.50 (-10.1%)	337.80 (-1.2%)
13.88	346.37	370.75 (+7.0%)	329.09 (-11.2%)	329.57 (-11.1%)
14.90	348.15	356.53 (+2.4)	323.93 (-9.1%)	317.50 (-10.9%)
16.63	300.50	320.70 (+6.7)	294.02 (-8.3%)	279.54 (-12.8%)

[1] (baseline CFD – baseline experiment)/ baseline experiment.
[1] (UTC 1 or 2 – baseline CFD)/baseline CFD.

5.2 Free surface

Free surface predictions for simulations in the critical hump region are shown in Figure 10, Figure 11, and Figure 12 for $U_{FS} = 11.89$, 12.88, and 14.90 respectively. From examining the figures and flow animations, it can be seen that unsteady and asymmetric overturning waves occur in the bow region at all speeds for the baseline and UTC 2 designs, and to a lesser extent for UTC 1. For the UTC 1 simulations, the bow wave tends to climb up the flat bottom bow section and form a more organized sheet before breaking, especially at the higher two speeds. Since the computational model does not include surface tension or sufficient resolution, the breakup of the bow sheet into individual spray droplets is not captured.

Results at the lower speed range of the hump region ($U_{FS} = 11.89$) in Figure 10 show smaller amplitudes, shorter wavelengths and a partially wetted transom face, consistent with Kelvin wavelength scaling. The baseline simulation shows a bow wave that is thrown forward in the axial direction, developing an unsteady recirculating plunging wave system. The UTC 1 and 2 simulations show less bow wave build up with smaller amplitude overturning waves. At the next higher speed ($U_{FS} = 12.88$), the baseline results in Figure 11 show a larger amplitude plunging bow wave and longer wavelength for the shoulder waves at the side of the ACV. The wave amplitude at the transom stern is much lower than that for the previous speed. However, the transom face remains partially wetted. At the higher end of the hump region ($U_{FS} = 14.90$), Figure 12 shows the highest amplitude unsteady breaking bow and shoulder waves for the baseline and UTC 2 cases, while the UTC 1 case shows quasi-steady overturning bow and shoulder waves. At this speed, the wave in transom region has dropped down to the transom flap so that the transom face is essentially dry. This also results in a large amplitude unsteady and asymmetric transom/rooster tail wave.

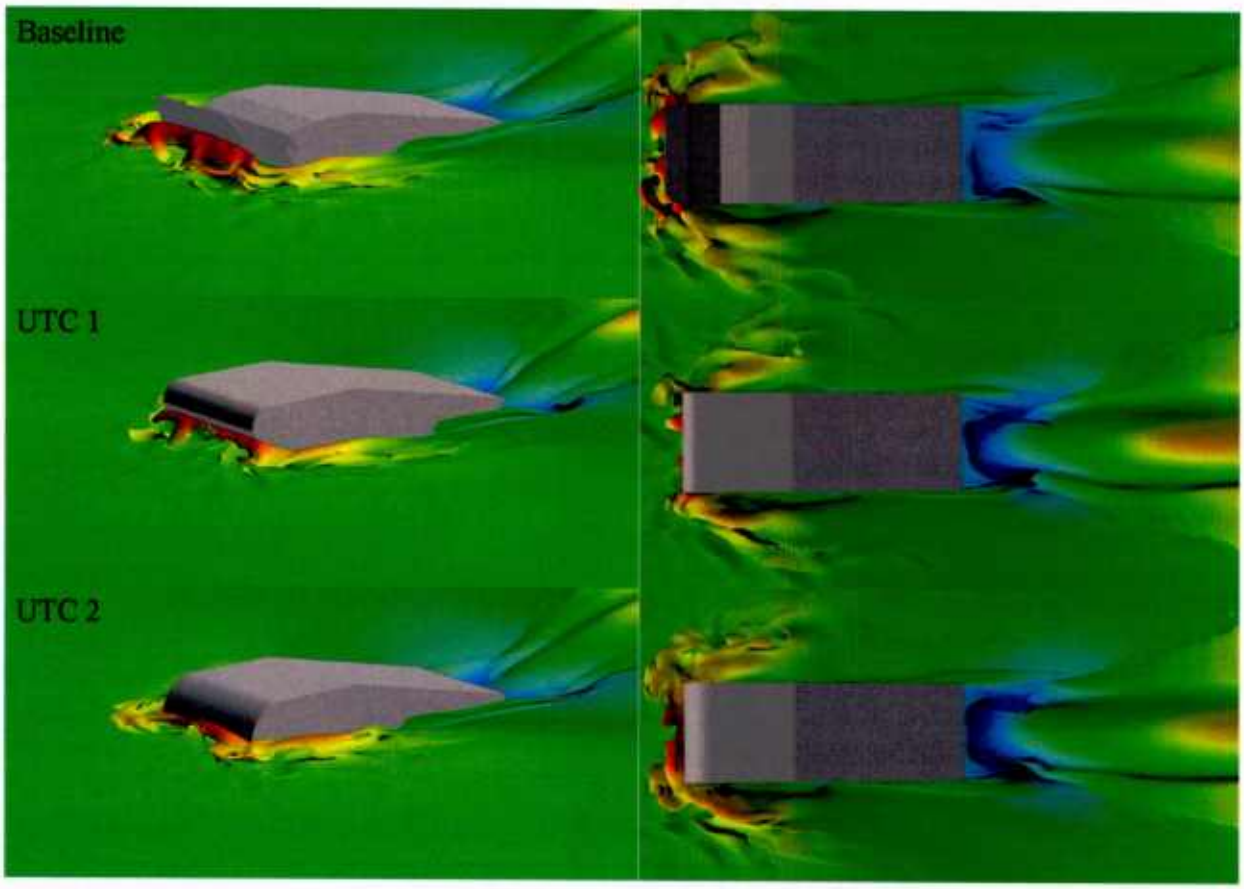

Figure 10. Comparison of free surface for ACV baseline, UTC 1 and UTC 2 cases, $U_{FS} = 11.89$.

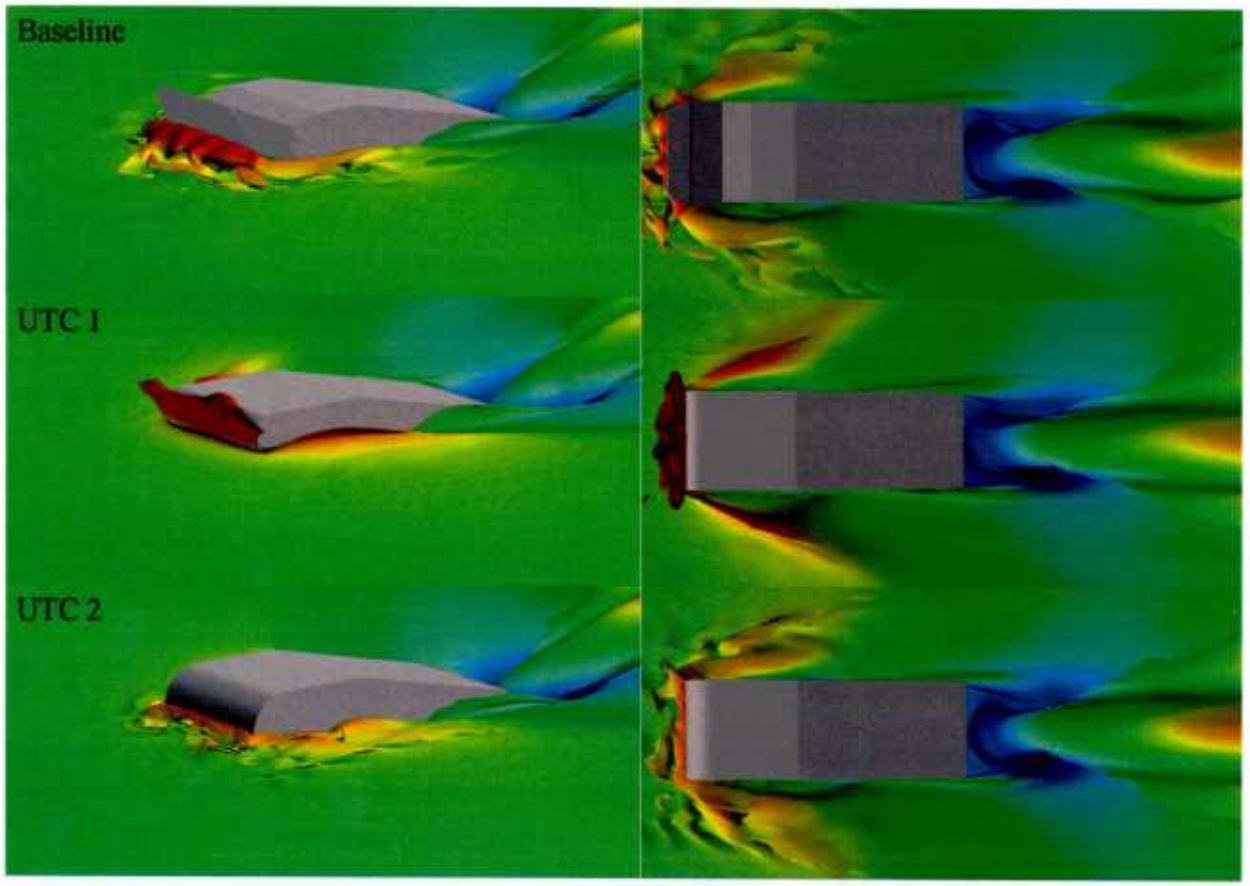

Figure 11. Comparison of free surface for ACV baseline, UTC 1 and UTC 2 cases, $U_{FS} = 12.88$.

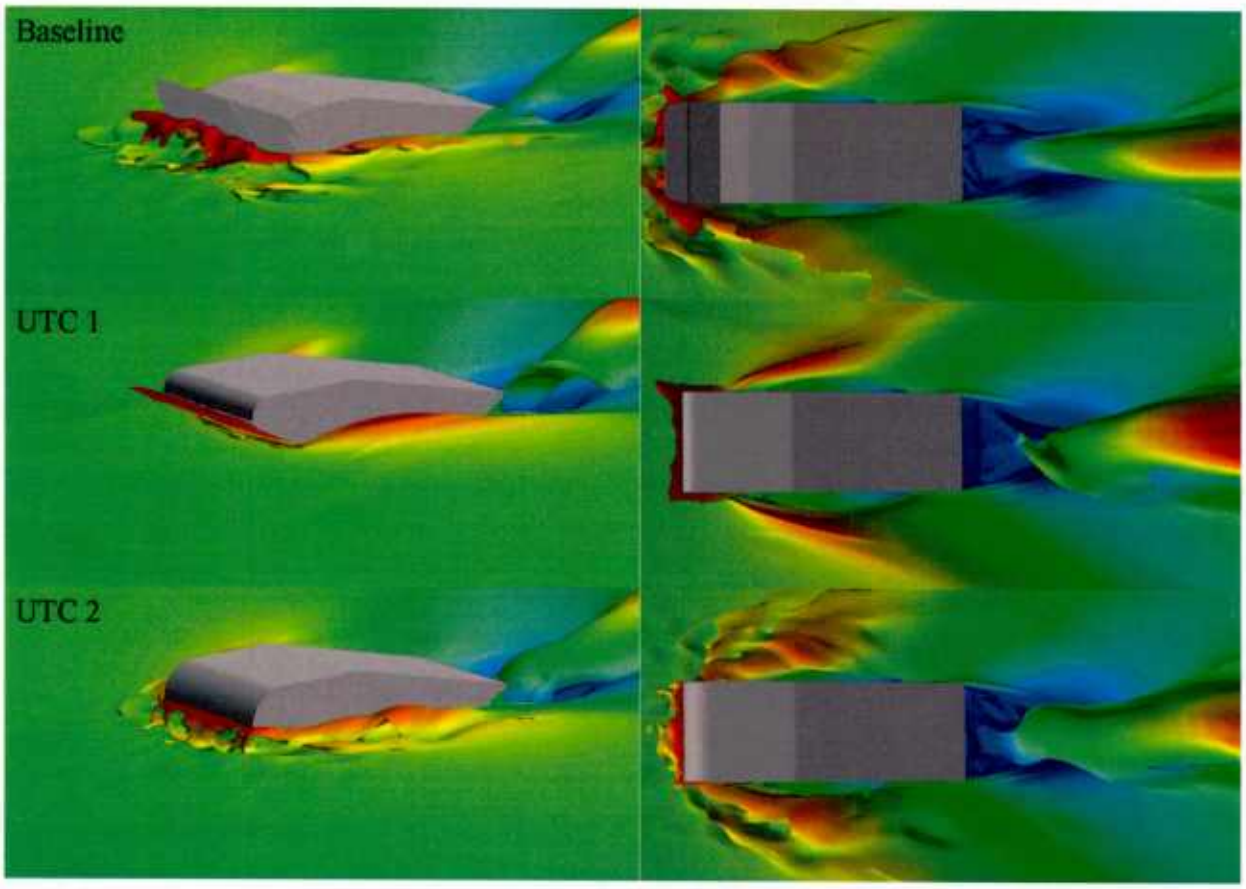

Figure 12. Comparison of free surface for ACV baseline, UTC 1 and UTC 2 cases, $U_{FS} = 14.90$.

6. SUMMARY AND RECOMMENDATIONS

National Center for Computational Engineering (SimCenter), University of Tennessee at Chattanooga, focused on the development of a computational procedure to evaluate various drag reduction strategies for hydrodynamically bluff-body vehicles. In particular, towards hydrodynamic drag reduction, different bow designs were investigated to replace the existing extendable bow vane of the current EFV configuration (designated as the Baseline ACV configuration in this report).

The *challenges* in this study and the *imposed constraints* to it were of particular note, as follows:

(1) As determined in a previous physical model-based assessment by the Naval Surface Warfare Center (NSWC), Carderock, in the "hump" region of total drag, generally, *only* about 6% of the total hydrodynamic drag of the Baseline ACV (*i.e.*, the current EFV) is due to friction; and the remaining 94% is largely *form drag*, together with wave drag. This is a very large departure from a ship hull designed from hydrodynamic drag considerations – for which, roughly 70% of the total drag would be due to friction, and the remainder would be the aggregate of form drag

and wave drag. For the Baseline ACV, therefore, a measurable reduction of form drag was needed towards a reduction of total drag.

(2) The principal constraint imposed by the research sponsor was that *no* modifications to the hull shape could be made aft of the bow shoulders, *i.e.*, aft of the leading edge of the track channel. (This constraint was imposed so that different bow shapes could be "bolted on" at the shoulders of a physical model for towing-tank tests.) This implied that the box-like shape of nearly the entire hull (responsible for the extreme level of form drag) could *not* be altered. Without this constraint, a large improvement in total resistance could have been realized.

Subject to the above constraint, SimCenter's approach to the hull geometry modification can be summarized as below:

(a) Initially, various bow concepts were examined, while maintaining the original length of Baseline ACV with bow vane retracted. None of these concepts resulted in a measurable reduction in total resistance as compared to the baseline configuration. This was due to the imposed constraint described in (2) above. (Towing-tank test data for Baseline ACV model were used to validate the computational procedure.)

(b) The next step was to determine the minimum bow length necessary for a measurable reduction of the hull total resistance. Free surface viscous computations were performed for a number of candidate bow designs to determine their effectiveness in drag reduction. It was determined that, under the constraint described in (2) above, the minimum bow length required for an appreciable decrease in resistance was two feet (model scale), *as measured from the fore end of the track channel.* This actually translates to an approximate length *decrease* of one foot as compared to Baseline ACV with its bow vane deployed.

(c) This approach resulted in two promising designs, referred to as UTC 1 and UTC 2 in this report. These designs resulted in an average drag reduction of 9.2% and 8.1%, respectively, over the "hump" region.

(d) It should be noted that, although the overall length of UTC 1 and UTC 2 is greater than that of Baseline ACV, the static waterline lengths of UTC 1 and UTC 2 are actually *less than that of Baseline ACV with bow plane deployed*, by 11% and 14% respectively. This is due to the shaping of the bow, together with the fact that, for the same estimated payload, the drafts of UTC 1 and UTC 2 are less than that of Baseline ACV.

(e) Calculations of the lift force and trim moment imbalances for UTC 1 and UTC 2 show that the computational models will tend to sink slightly and rotate bow down to achieve dynamic equilibrium, relative to the baseline orientation. This could further reduce drag in the "hump" region.

Based on these results, it is anticipated that physical model tests of either the UTC 1 or 2 geometries would result in drag reduction relative to the baseline configuration. If down selection to one design is required for model testing, the UTC 1 geometry would provide an acceptable starting point.

It is recommended that a more comprehensive study of modifying the current vehicle be undertaken *removing* the restriction of no geometric modifications aft of the bow shoulders to determine to what extent the overall drag could be reduced using traditional naval architecture principles. *As stated previously, without this imposed restriction, a large improvement in total resistance could have been realized.*

7. REFERENCES

Hyams, D.G., Sreenivas, K., Pankajakshan, R., Nichols, III, D.S., Briley, W.R., and Whitfield, D.L., "Computational simulation of model and full scale Class 8 trucks with drag reduction devices," Computers & Fluids, Volume 41, Issue 1, February 2011, Pages 27-40.

Lee, D., Maki, K., Wilson, R., Troesch, A., and Vlahopoulos, N., "Dynamic Response of a Marine Vessel Due to Wave-Induced Slamming," Int. Sym. On Vibro-Impact Dynamics of Ocean Systems and Related Problems, Troy, Michigan, 2-3 Oct. 2008.

Nichols, D. S., "Development of a Free Surface Method Utilizing an Incompressible Multi-Phase Algorithm to Study the Flow About Surface Ships and Underwater Vehicles," Ph.D. Dissertation, Mississippi State University, August 2002.

Noack R., "SUGGAR: A General Capability for Moving Body Overset Grid Assembly," AIAA Paper 2005-5117, 17th AIAA Computational Fluid Dynamics Conf., Toronto, Ontario, Canada, 2005.

Wilson, R.V., Nichols, D.S., Mitchell, B., Karman, S.L., Hyams, D.G., Sreenivas, K., Taylor, L.K., Briley, W.R., and Whitfield, D.L., "Application of an Unstructured Free Surface Flow Solver for High Speed Transom Stern Ships," 26th Symposium on Naval Hydrodynamics, Rome Italy, Sept. 2006.

Wilson, R.V., Nichols, D.S., Mitchell, B., Karman, V. Betro, S.L., Hyams, D.G., Sreenivas, K., Taylor, L.K., Briley, W.R., and Whitfield, D.L., "Simulation of a Surface Combatant with Dynamic Ship Maneuvers," 9th Int. Conf. on Numerical Ship Hydrodynamics, Ann Arbor, Michigan, Aug. 2007.

Wilson, R., Lei, J., Karman, Jr., S.L., Hyams, D., Sreenivas, K., Taylor, L., and Whitfield D., 2008, "Simulation of Large Amplitude Ship Motions for Prediction of Fluid-Structure Interaction," Proceedings of the 27th ONR Symposium on Naval Hydrodynamics, Seoul, Korea, 5-10 Oct. 2008.